Advances in Concrete Construction, *Vol. 8, No. 1 (2019) 1-7*
DOI: https://doi.org/10.12989/acc.2019.8.1.001

Use of waste glass as coarse aggregate in concrete: mechanical properties

Lan-lan Yan[1] and Jiong-Feng Liang[*2]

[1]*Faculty of Science, East China University of Technology, Nanchang 330013, China*
[2]*Faculty of Civil & Architecture Engineering, East China University of Technology, Nanchang 330013, China*

(Received August 17, 2018, Revised April 5, 2019, Accepted April 9, 2019)

Abstract. The possibility of using recycled coarse glass aggregates as a substitute for natural crushed stone are relatively limited. In order to promote it for engineering application, this paper reports the effect of coarse glass aggregate on mechanical behavior of concrete. The coarse aggregates are substituted for coarse glass aggregate (CGA) as 0%,20%,40%,60%,80% and 100%.The results show that increasing the coarse glass aggregate content cause decrease in compressive strength, the elastic modulus, the splitting tensile strength, the flexural strength. An equation is presented to generate the relationship between cube compressive strength and prism compressive strength, the relationship between cube compressive strength and elastic modulus, the relationship between cube compressive strength and splitting tensile strength, the relationship between cube compressive strength and flexural strength of coarse glass concrete.

Keywords: coarse glass aggregate; concrete; mechanical behavior; relation

1. Introduction

For recent decades, environment pollution and wasting of resources from glass waste has caused a great consideration of the whole society. It is necessary to find a proper method to recycle the glass waste. Using the glass in addition or replacement of natural aggregate in concrete can protect the environment and help develop a new kind of concrete. So some authors have studied the use of waste glass as aggregates in concrete (Kim *et al*. 2018, Chiou *et al*. 2014, Jani and Hogland 2014, Taha and Nounu 2009).

Yang *et al.* (2018) investigated the generation of cracks during ASR development of glass aggregate concrete by using the wet-mix and dry-mix methods. Lee *et al.* (2018) studied mechanical properties and durability of concrete incorporating glass powder and glass sludge wastes as supplementary cementing material. Choi *et al.* (2018) studied the characteristics of volume change and heavy metal leaching in mortar specimens recycled heavyweight waste glass as fine aggregate. Hajimohammadi *et al.* (2018) studied the thermal and mechanical properties of geopolymer foams with glass fines versus sand as aggregates. Du and Tan (2017) investigated mechanical and durability properties of concrete with cement replaced by finely grounded glass powder in high volume up to 60%. Nader *et al.* (2017) studied the effects of recycled concrete aggregate and waste glass on the properties of concrete. Kim *et al.* (2017) studied the effects of particle size and cement replacement of liquid crystal display (LCD) glass powder in concrete. Ziari *et al.* (2017) studied the effect of temperature on skid resistance of concrete pavements containing crushed glass. Letelier *et al.* (2017) studied the mechanical behavior of concrete with recycled aggregates from precast debris and waste glass. They found that the combination of both recycled materials permits an increased amount of recycled coarse aggregates reducing the loss of mechanical performance of the concrete, and enhances the environmental value of the final material. Kao *et al.* (2017) developed a multivariable prediction model for the determination of waste LCD glass concrete compressive strength. Wang (2017) established a prediction model for the electrical resistivity of self-consolidating concrete by using waste LCD (liquid crystal display) glass as part of the fine aggregate. Pourabbas *et al.* (2016) evaluated the advantages of adding recycled glass powder (RGP), crumb Rubber (CR), styrene-butadiene rubber (SBR) and styrene butadiene styrene (SBS) to base bitumen with grade of 60/70 for modification of asphalt concrete. Liang *et al.* (2015) studied compressive strength and the stress-strain curve (SSC) of recycled fine glass aggregate concrete with different replacement percentages of recycled fine glass aggregate.

In this study, the effects of coarse glass aggregates as a substitute for natural crushed stone in concrete on the compressive strength, elastic modulus, splitting tensile strength, flexural strength were investigated.

2. Experimental programme

2.1 Materials

An ordinary P.O.32.5R Portland cement with a density of 3050 kg/m^3 was used, which was compatible with Chinese Standard “GB175-2007”. The chemical composition of ordinary Portland cement is stated in Table 1. The river sand with a 4.75 mm maximum size and a apparent density of 2570 kg/m^3 was used as fine aggregate,

∗Corresponding author, Ph.D.
E-mail: jiongfeng108@126.com

http://www.techno-press.org/?journal=acc&subpage=7 ISSN: 2287-5301 (Print), 2287-531X (Online)

Table 1 Chemical composition of ordinary Portland cement (%)

Lime (Cao)	Silica (SiO_2)	Alumina (Al_2O_3)	Ironoxide (Fe_2O_3)	Sodium oxide (Na_2O)	Magnesium oxide(MgO)	Potassium oxide(K_2O)	Sulfur Trioxide ($S0_3$)	Loss on ignition
56.62	22.98	6.95	3.72	4.15	1.95	0.93	1.48	1.22

(a) Crushed stone

(b) Coarse glass aggregate

Fig. 1 Different coarse aggregate used in the concrete mixture

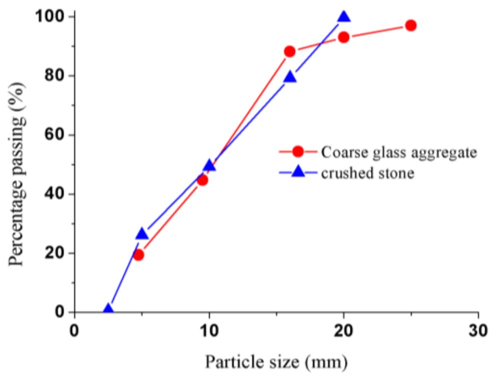

Fig. 2 Grading curves of crushed stone and coarse glass aggregate

Table 2 Chemical composition of coarse glass aggregate (%)

Silica (SiO_2)	Sodium oxide (Na_2O)	Magnesium oxide (MgO)	Alumina (Al_2O_3)	Iron oxide (Fe_2O_3)	Lime (Cao)	Potassium oxide (K_2O)
72.32	12.18	2.29	0.78	0.14	12.05	0.24

Table 3 Physical properties of river sand

Fineness modulus	Bulk density (kg/m^3)	Apparent density (kg/m^3)	Silt content (%)
2.6	1460	2570	1.56

Table 4 Physical properties of crushed stone

Grading (mm)	Bulk density (kg/m^3)	Apparent density (kg/m^3)	Water absorption (%)	Silt content (%)	Crushing value (%)
5-20	1610	2755	0.5	3.9	8.4

Table 5 Physical properties of coarse glass aggregate

Bulk density (kg/m^3)	Apparent density (kg/m^3)	Water absorption (%)	Void ratio (%)
1575	2505	0.19	47

Table 6 Mix proportion of coarse glass aggregate concrete

Index	Glass content (%)	Glass ($kg\cdot m^{-3}$)	Cement ($kg\cdot m^{-3}$)	Sand ($kg\cdot m^{-3}$)	Stone ($kg\cdot m^{-3}$)	Water ($kg\cdot m^{-3}$)
G0	0	0	443	564	1198	195
G20	20	240	443	564	958	195
G40	40	479	443	564	719	195
G60	60	719	443	564	479	195
G80	80	958	443	564	240	195
G100	100	1198	443	564	0	195

which meted Chinese Standard "GBT14684-2011". Two types of coarse aggregate were used in the concrete mixtures. One of coarse aggregate was natural common crushed stone having the maximum size of 20mm, which meted Chinese Standard "GBT14684-2011".The second type was coarse glass aggregate (CGA) having the maximum size of 25 mm, which also meted Chinese Standard "GBT14684-2011". Fig. 1 gives the photos of crushed stone and coarse glass aggregate samples used in the concrete mixture. Fig. 2 shows the grading curves of crushed stone and coarse glass aggregate. Table 2 lists the chemical composition of coarse glass aggregate. The Physical properties of river sand, crushed stone and coarse glass aggregate are shown in Tables 3, 4, 5, respectively.

2.2 Mix proportions

Six concrete mixture proportions having water/cement ratio of 0.44 were prepared. First was the control mix (without CGA) and the other five mixtures contained CGA. In the concrete mixture proportions, coarse aggregate (common crushed stone was replaced with CGA by weight. The proportion of coarse aggregate replaced were 20%, 40%, 60%, 80% and 100%. The design of the concrete mix is given in Table 6.

2.3 Specimen preparation and curing

All mixing was conducted under laboratory conditions. The dry cement and aggregates were mixed for 1min in a 0.05 m^3 laboratory mixer. The mixing continued for further 1 min while about 70% of water was added. The mixing was continued for another 1 min. Before casting the specimens, the slump test of the mixture was performed to determine its workability. In total, 90 concrete specimens were prepared. For each mixture, three 150×150×150 mm cubes, three 150×150×300 mm prisms, three 150×150×300

Table 7 Test results

Properties	Mix Code	Experimental test results (Mpa)			Mean (Mpa)	Standard deviation (Mpa)	Coefficient of variation (%)
		Specimen No.1	Specimen No.2	Specimen No.3			
Cube compressive strength	G0	30.1	31.2	31.5	30.9	0.74	2.38
	G20	27.5	28.1	29.2	28.3	0.86	3.05
	G40	27.1	26.9	27.6	27.2	0.36	1.33
	G60	26.9	26.2	26.5	26.5	0.35	1.32
	G80	25.7	26.1	25.6	25.8	0.26	1.03
	G100	18.2	18.9	19.0	18.7	0.44	2.33
Prism compressive strength	G0	23.4	22.9	23.1	23.1	0.25	1.09
	G20	20.8	22.5	21.8	21.7	0.85	3.94
	G40	20.5	21.8	20.9	21.1	0.67	3.16
	G60	20.1	21.4	21.0	20.8	0.67	3.20
	G80	19.8	20.4	20.9	20.4	0.55	2.70
	G100	16.5	16.1	17.1	16.6	0.50	3.04
Modulus of elasticity	G0	28873	28867	28872	28871	3.21	0.01
	G20	27568	27570	27570	27569	1.15	0.00
	G40	26430	26436	26430	26432	3.46	0.01
	G60	26185	26190	26186	26187	2.65	0.01
	G80	25982	25988	25989	25986	3.79	0.01
	G100	23486	23484	23491	23487	3.61	0.02
Splitting tensile strength	G0	2.31	2.28	2.35	2.31	0.04	1.52
	G20	2.18	2.19	2.14	2.17	0.03	1.22
	G40	2.11	2.12	2.09	2.11	0.02	0.73
	G60	2.06	2.09	2.07	2.07	0.02	0.74
	G80	2.02	2.04	2.05	2.04	0.02	0.75
	G100	1.64	1.66	1.63	1.64	0.02	0.93
Flexural strength	G0	3.59	3.61	3.63	3.61	0.02	0.55
	G20	3.47	3.46	3.45	3.46	0.01	0.29
	G40	3.40	3.37	3.40	3.39	0.02	0.51
	G60	3.33	3.39	3.32	3.35	0.04	1.13
	G80	3.31	3.35	3.27	3.31	0.04	1.21
	G100	2.81	2.84	2.79	2.81	0.03	0.89

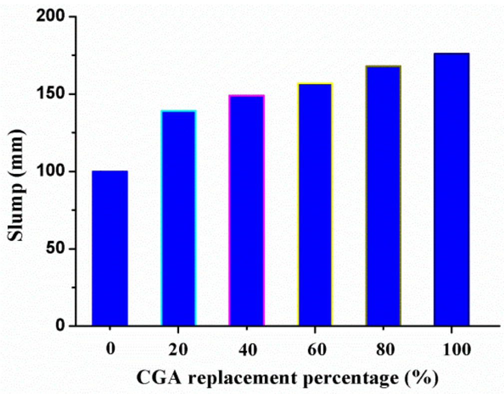

Fig. 3 Slump of concrete

mm cubes, three 150×150×150 mm cubes, three 150×150×550 mm prisms were used for the study of cube compressive strength, prism compressive strength, modulus of elasticity, splitting tensile strength and flexural strength. After 24 h, the specimens were demoulded and cured in a fog room (20±2℃, 95% relative humidity) for 28 days. All specimens were tested according to Standard for test method of mechanical properties on ordinary concrete in china (GB/T 50081-2010) after 28 days.

3. Results and discussion

3.1 Workability of fresh concrete

The slump test results of concrete are shown in Fig. 3. The workability of fresh CGA concrete increased with an increase in coarse glass aggregate replacement percentage. The coarse glass aggregate replacement percentage from 0% to 20%, 40%, 60%, 80% and 100% increased the workability about 39%, 49%, 57%, 68% and 76%,respectively. The higher workability of CGA concrete may be attributed to the relative smooth surface texture of coarse glass aggregate.

3.2 Compressive strength

Table 7 demonstrates the compressive strength of all test specimens. There was a reduction in the compressive strength of concrete mixtures with the coarse glass aggregate as replacement of regular coarse aggregate. The cube compressive strength of control mixture G0 (0% CGA) was 30.9 MPa, whereas mixture G20 (20% CGA), G40 (40% CGA), G60 (60% CGA), G80 (80% CGA) and G100 (100% CGA) achieved strength of 28.3 MPa, 27.2

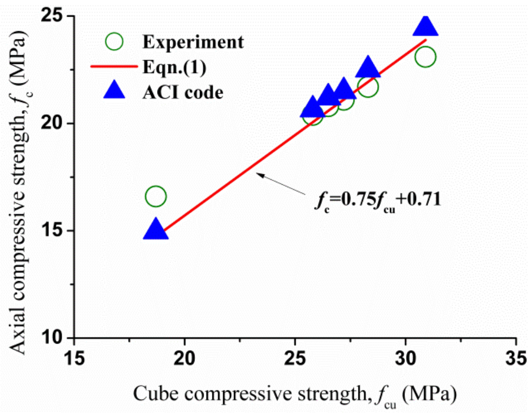

Fig. 4 Relationship between cube and axial compressive strength

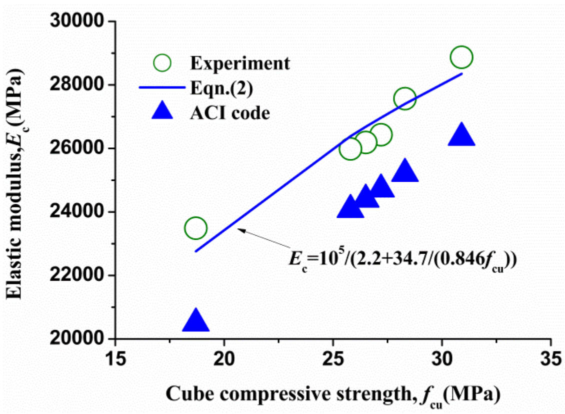

Fig. 5 Relationship between cube compressive strength and elastic modulus

MPa, 26.5 MPa, 25.8 MPa and 18.7 MPa, respectively; a decrease of 8.4%, 11.9%, 14.2%, 16.5% and 39.5% in comparison with the cube compressive strength of control mixture G0 (0% CGA). And increasing the coarse glass aggregate replacement percentage from 0% to 20%, 40%, 60%, 80% and 100% decreased the prism compressive strength by about 8.4%, 11.9%, 14.2%, 16.5% and 39.5%, respectively.

The decrease in compressive strength with the addition of CGA could probably due to the fact that coarse glass aggregates were more brittle than regular coarse aggregates, and also due to the worse bond between the coarse glass aggregate and the matrix.

According to the test data, a relationship between the prism compressive strength and cube compressive strength was suggested

$$f_c = 0.75 f_{cu} + 0.71 \tag{1}$$

where f_c and f_{cu} are the prism compressive strength and cube compressive strength both in MPa, respectively.

Fig. 4 demonstrates the relationship between cube and axial compressive strength. Comparisons of the experimental and the predicted values by Eq. (1) presented in Fig. 4, it show that Eq. (1) fit the experimental results satisfactorily. The predicted axial compressive strength using ACI code (2002) is compared with the test result in Fig. 4. Generally, ACI code predicted axial compressive strength slightly higher than the test result.

3.3 Elastic modulus

Table 7 also presents the elastic modulus of all test specimens. It can be seen that replacement of coarse aggregate with CGA reduced elastic modulus of concrete mixtures. The value of elastic modulus of mixture G0 (0% CGA),G20 (20% CGA), G40 (40% CGA), G60 (60% CGA), G80 (80% CGA) and G100 (100% CGA) was 28871 MPa, 27569 MPa, 26432 MPa, 26187 MPa, 25986 MPa and 23487 MPa, respectively. Compared to control mixture G0 (0% CGA), the rate of decrease of elastic modulus for mixture G20 (20% CGA), G40 (40% CGA), G60 (60% CGA), G80 (80% CGA) and G100 (100% CGA) was 4.5%, 8.4%, 9.3%, 10% and 18.6%, respectively.

A relationship between the elastic modulus and cube compressive strength was suggested

$$E_c = \frac{10^5}{2.2 + \dfrac{34.7}{0.846 f_{cu}}} \tag{2}$$

where E_c and f_{cu} are the elastic modulus and cube compressive strength both in MPa, respectively.

This can be shown in Fig. 5 that demonstrates the relationship between elastic modulus and cube compressive strength. It could be observed that the experiment data agree relatively well with Eq. (2). As shown in Fig. 5, ACI code underestimated the values of elastic modulus.

3.4 Splitting tensile strength

The splitting tensile strength of concrete mixtures is shown in Table 7. Like compressive strength and elastic modulus, splitting tensile strength of concrete mixtures decreased with the increase in the replacement percentage of coarse glass aggregate. By increasing the replacement percentage of coarse glass aggregate from 0% to 100%, the splitting tensile strength decreased from 2.31 MPa to 1.64 MPa. Compared to control mixture G0 (0% CGA), the rate of decrease of splitting tensile strength for mixture G20 (20% CGA), G40 (40% CGA), G60 (60% CGA), G80 (80% CGA) and G100 (100% CGA) was 6.1%, 8.7%, 10.4%, 11.7% and 29%, respectively.

The proposed equation for a relationship between the splitting tensile strength and cube compressive strength was given

$$f_{st} = 0.22 f_{cu}^{0.68} \tag{3}$$

where f_{st} and f_{cu} are the splitting tensile strength and cube compressive strength both in MPa, respectively.

Fig. 6 shows the relationship between splitting tensile strength and cube compressive strength. It was clear that the test data agree relatively well with Eq. (3). It can be seen from Fig. 6, the predicted splitting tensile strength using ACI code was lower than the test results.

3.5 Flexural strength

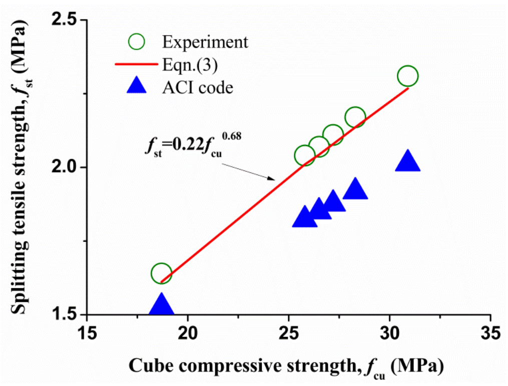

Fig. 6 Relationship between cube compressive strength and splitting tensile strength

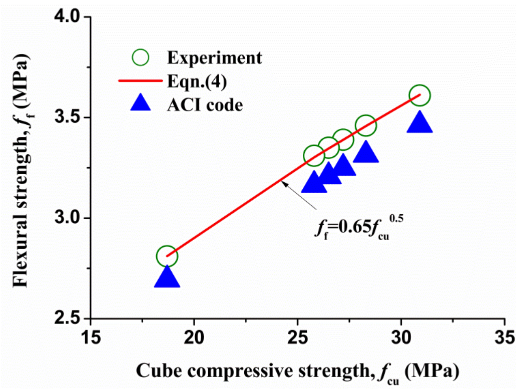

Fig. 7 Relationship between cube compressive strength and flexural strength

The flexural strength of concrete mixtures is shown in Table 7. When the replacement percentage of coarse glass aggregate increased from 0% to 100%, the flexural strength decreased from 3.61 MPa to 2.81 MPa. The rate of decrease for mixture G20 (20% CGA), G40 (40% CGA), G60 (60% CGA), G80 (80% CGA) and G100 (100% CGA) was 4.2%, 6.1%, 7.2%, 8.3% and 22.2%, respectively. This means that the coarse glass aggregate obviously reduced the flexural strength of concrete mixtures.

The proposed equation for a relationship between the flexural strength and cube compressive strength was given

$$f_f = 0.65 f_{cu}^{0.5} \tag{4}$$

where f_f and f_{cu} are the flexural strength and cube compressive strength both in MPa, respectively.

Fig. 7 shows the relationship between flexural strength and cube compressive strength. It was clear that the test data agree relatively well with Eq. (4). As shown in Fig. 7, the flexural strengths were under-predicted using ACI code.

3.6 Stress-strain curves

Fig. 8 shows the typical stress–strain curves of different replacement percentage of coarse glass aggregate concrete. It can be seen that all coarse glass aggregate concrete present very similar pattern of the stress–strain curves. The value of the peak strain corresponding to the peak stress was lower for coarse glass aggregate concrete compared to

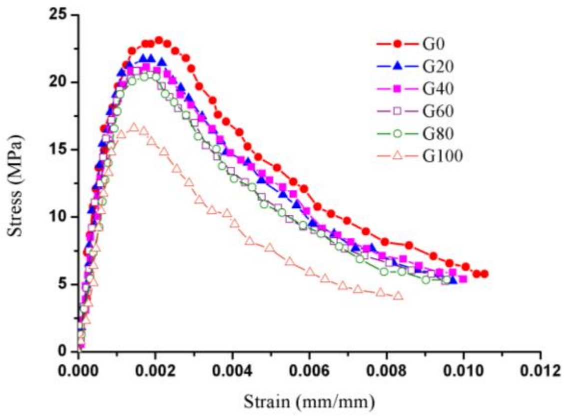

Fig. 8 Typical stress-strain curves

that of natural coarse aggregate concrete. This may be due to the lower elastic modulus of coarse glass aggregate concrete compared to that of natural coarse aggregate concrete as shown in Table 4. The ultimate strain is taken as the axial strain beyond the peak stress at a stress level equal to 85% of the peak stress. It can be seen from Fig. 6 that the replacement of coarse aggregate with CGA to natural coarse aggregate for the concrete decreases the ultimate strain.

In an attempt to find an equation to describe the complete stress–strain relationship, Guo and Zhang (1982) had suggested the following expression

$$y = \begin{cases} ax + (3-2a)x^2 + (a-2)x^3, 0 \le x < 1 \\ \dfrac{x}{b(x-1)^2 + x}, x \ge 1 \end{cases} \tag{5}$$

where $x=\varepsilon/\varepsilon_0$, $y=\sigma/f_c$; ε is the strain, ε_0 is the peak strain, σ is the stress, f_c is the peak stress, a and b are constants to be determined.

In the form of Eq. (5), according to the experiment results, the parameters a and b were obtained by a data regression analysis. The results are given as follows

$$a = 0.4r^2 - 1.61r + 2.79 \tag{6}$$

$$b = 0.8r^2 - 0.93r + 0.85 \tag{7}$$

where r is the coarse glass aggregate replacement percentage.

As shown in Fig. 9, the theoretical curves exhibit a good agreement with the experimental curves. So, the approximate stress-strain relations for the coarse glass aggregate concrete can be used for the structure analysis and design in the application of coarse glass aggregate concrete.

5. Conclusions

The following conclusions are drawn from this study:

- The workability of coarse glass aggregate concrete increases by increasing the replacement percentage of coarse glass aggregate. The maximum enhancement of about 76% was obtained for CGA concrete with 100% coarse glass aggregate content.

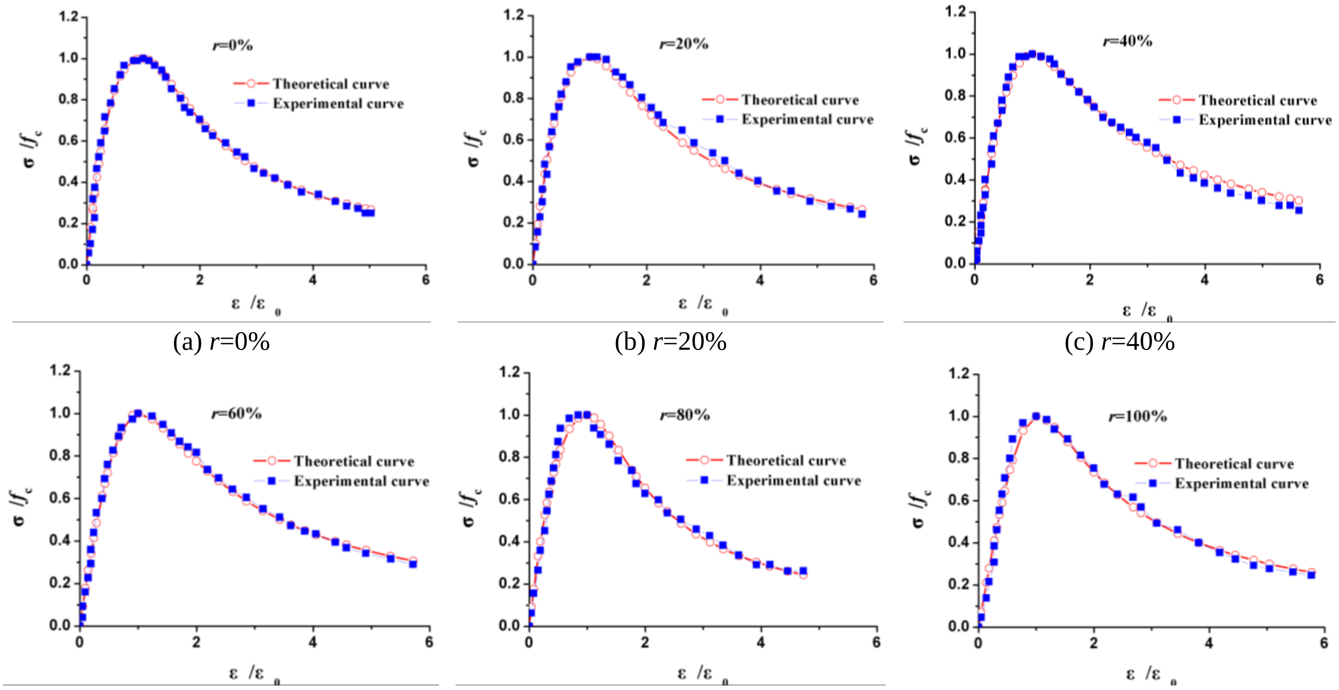

(a) *r*=0% (b) *r*=20% (c) *r*=40%

(d) *r*=60% (e) *r*=80% (f) *r*=100%

Fig. 9 Comparison of the normalized stress–strain curves

• The compressive strength of coarse glass aggregate concrete decreases with an increase in coarse glass aggregate. It could probably due to the worse bond between the coarse glass aggregate and the matrix. Like compressive strength, the elastic modulus decreases with the increasing percentage o f substitution of coarse glass aggregates.

• The substitution of coarse glass aggregates decreases the splitting tensile strength. By increasing the replacement percentage of coarse glass aggregate from 0% to 100%, the splitting tensile strength decreased from 2.31 MPa to 1.64 MPa.

• The substitution of coarse glass aggregates decreases the flexural strength. When the replacement percentage of coarse glass aggregate increased from 0% to 100%, the flexural strength decreased from 3.61 MPa to 2.81 MPa.

• An equation is presented to generate the relationship between cube compressive strength and prism compressive strength, the relationship between cube compressive strength and elastic modulus, the relationship between cube compressive strength and splitting tensile strength, the relationship between cube compressive strength and flexural strength of coarse glass concrete.

• The formula of Guo and Zhang' stress-strain curve for normal concrete was extended to coarse glass aggregate concrete, which agreed well with the test results.

Acknowledgments

This work was supported by the Chinese National Natural Science Foundation (No. 51868001), the Natural Science Foundation of Jiangxi Province for Distinguished Young Scholars (No. 20162BCB23051), the Natural Science Foundation of Jiangxi Province (No. 20171BAB206053), which are gratefully acknowledged.

References

ACI 318-02(2002), Building Code Requirement for Reinforced Concrete Structures (ACI 318-02) and Commentary (ACI 318R-02), American Concrete Institute, Detroit.

Chinese Code for the Design of Reinforced Concrete Structures (GB50010) (2010), Chinese Building Construction Publishing Press, Beijing. (in Chinese)

Chiou, I.J., Chen, C.H. and Lin, C.L. (2014), "Performance of adding waste glass and sewage sludge to reservoir-sediment aggregates", *Comput. Concrete*, **13**(1), 83-96. https://doi.org/10.12989/cac.2014.13.1.083.

Choi, S.Y., Choi, Y.S. and Yang, E.I. (2018), "Characteristics of volume change and heavy metal leaching in mortar specimens recycled heavyweight waste glass as fine aggregate", *Constr. Build. Mater.*, **165**, 424-433. https://doi.org/10.1016/j.conbuildmat.2018.01.050.

Common Portland Cement (GB175-2007), Chinese Building Construction Publishing Press, Beijing. (in Chinese)

Du, H.J. and Tan, K.H. (2017), "Properties of high volume glass powder concrete", *Cement Concrete. Compos.*, **75**, 22-26. https://doi.org/10.1016/j.cemconcomp.2016.10.010.

Guo, Z.H. and Zhang, X.Q. (1982), "Experimental investigation of stress-strain curves for concrete", *Chin. J. Build. Struct.*, **3**(1), 1-12. (in Chinese)

Hajimohammadi, A., Ngo, T. and Kashani, A. (2018), "Sustainable one-part geopolymer foams with glass fines versus sand as aggregates", *Constr. Build. Mater.*, **171**, 223-231. https://doi.org/10.1016/j.conbuildmat.2018.03.120.

Jani, Y. and Hogland, W. (2014), "Waste glass in the production of cement and concrete-A review", *J. Environ. Chem. Eng.*,

2(3), 1767-1775. https://doi.org/10.1016/j.jece.2014.03.016.

Kao, C.H., Wang, C.C. and Wang, H.Y. (2017), “A neural-based predictive model of the compressive strength of waste LCD glass concrete”, *Comput. Concrete*, **19**(5), 457-465. https://doi.org/10.12989/cac.2017.19.5.457.

Kim., S., Hanif, A. and Jang, I. (2018), “Incorporating liquid crystal display (LCD) glass waste as supplementary cementing material (SCM) in cement mortars-rationale based on hydration, durability, and pore characteristics”, *Mater.*, **11**(12), 2538. https://doi.org/10.3390/ma11122538.

Kim., S.K., Kang, S.T., Kim, J.K. and Jang, I.Y. (2017), “Effects of particle size and cement replacement of LCD glass powder in concrete”, *Adv. Mater. Sci. Eng.*, **2017**, Article ID 3928047, 12. https://doi.org/10.1155/2017/3928047.

Lee, H., Hanif, A., Usman, M., Sim, J. and Oh, H. (2018), “Performance evaluation of concrete incorporating glass powder and glass sludge wastes as supplementary cementing material”, *J. Clean. Prod.*, **170**, 683-693. https://doi.org/10.1016/j.jclepro.2017.09.133.

Letelier, V., Tarela, E., Osses, R., Cárdenas, J.P. and Moriconi, G. (2017), “Mechanical properties of concrete with recycled aggregates and waste glass”, *Struct. Concrete*, **18**(1), 40-53. https://doi.org/10.1002/suco.201500143.

Liang, J.F., Yang, Z.P., Yi, P.H. and Wang, J.B. (2015), “Mechanical properties of recycled fine glass aggregate concrete under uniaxial loading”, *Comput. Concrete*, **16**(2), 275-285. https://doi.org/10.12989/cac.2015.16.2.275.

Nader, B., Mahmoud, N., Seyed Mahdi, H., Mehrdad, R., Siavash, A. and Parisa, R. (2017), “Modelling and optimisation of concrete containing recycled concrete aggregate and waste glass”, *Mag. Concrete. Res.*, **69**(6), 306-316. http://dx.doi.org/10.1680/jmacr.16.00279.

Pourabbas, B.M., Marandi, S.M. and Ghasemi, F. (2016), “Effect of recycled glass powder on asphalt concrete modification”, *Struct. Eng. Mech.*, **59**(2), 373-385. http://dx.doi.org/10.12989/sem.2016.59.2.373.

Sand for Cinstruction (GBT14684-2011), Chinese Building Construction Publishing Press, Beijing. (in Chinese)

Taha, B. and Nounu, G. (2009), “Utilizing waste recycled glass as sand/cement replacement in concrete”, *J. Mater. Civil Eng.*, **21**(12), 709-721. https://doi.org/10.1061/(ASCE)0899-1561(2009)21:12(709).

Wang, C.C. (2017), “Prediction model of resistivity and compressive strength of waste LCD glass concrete”, *Comput. Concrete*, **19**(5), 467-475. https://doi.org/10.12989/cac.2017.19.5.467.

Yang, S.Q, Cui, H.Z. and Poon, H.Z. (2018), “Assessment of in-situ alkali-silica reaction (ASR) development of glass aggregate concrete prepared with dry-mix and conventional wet-mix methods by X-ray computed micro-tomography”, *Cement Concrete. Compos.*, **90**, 266-276. https://doi.org/10.1016/j.cemconcomp.2018.03.027.

Ziari, H., Barakoohi, A.T. and Moniri, A. (2017), “Laboratory investigation of the effect of temperature on frictional properties of concrete pavements containing crushed glass”, *Int. J. Pav. Res. Technol.*, **10**(4), 297-303. https://doi.org/10.1016/j.ijprt.2017.04.006.

CC